Article

Single-Crystal-to-Single-Crystal Transformation from δ-(BEDT-TTF)$_4$[OsNOCl$_5$]$_{1.33}$(C$_6$H$_5$NO$_2$)$_{0.67}$ to β″-(BEDT-TTF)$_3$[OsNOCl$_5$]

Leokadiya Zorina [1,*]**, Sergey Simonov** [1]**, Enric Canadell** [2] **and Rimma Shibaeva** [1]

[1] Institute of Solid State Physics RAS, Chernogolovka MD 142432, Russia;
   E-Mails: simonovsv@rambler.ru (S.S.); shibaeva@issp.ac.ru (R.S.)

[2] Institut de Ciència de Materials de Barcelona (ICMAB-CSIC), Campus de la UAB,
   Bellaterra 08193, Spain; E-Mail: canadell@icmab.es

* Author to whom correspondence should be addressed; E-Mail: zorina@issp.ac.ru;
   Tel.: +7-496-522-8386; Fax: +7-496-522-8160.

Abstract: We report on the single-crystal-to-single-crystal transformation occurring over time in a layered organic molecular conductor based on BEDT-TTF. The process is connected with removal of solvent molecules from the complex anion layer resulting in concomitant partial irreversible conversion of the δ-(BEDT-TTF)$_4$[OsNOCl$_5$]$_{1.33}$(C$_6$H$_5$NO$_2$)$_{0.67}$ structure to the β″-(BEDT-TTF)$_3$[OsNOCl$_5$] structure. Along with symmetry lowering from *I*2/*a* to *P*$\bar{1}$, huge, drastic changes in the conducting BEDT-TTF layer as well as in the anion arrangement are observed, meanwhile crystallinity of the sample is retained. Coexistence of two phases, parent δ and daughter β″ in the same crystal helps in the study of their mutual orientation as well as to formulate a mechanism for the structural transformation.

Keywords: single-crystal-to-single-crystal transformation; low-dimensional organic conductors; BEDT-TTF; photochromic octahedral anion; single crystal structure; electronic band structure

1. Introduction

Hybrid radical cation salts based on different π-organic donors with the inorganic photochromic metal complex anions $[MNOX_5]^{2-}$ (M = Fe, Ru, Os; X = CN, Cl, Br) have recently been the object of considerable interest [1–20]. Such hybrid molecular solids combine conducting properties of the organic component and specific characteristics of the inorganic network and show wide variation in composition, stoichiometry and packing of conducting radical cation layers. In particular, the use of the $[OsNOX_5]^{2-}$ anion in syntheses of the BEDT-TTF [bis(ethylendithio)terathiafulvalene] radical cation salts has produced a family of conductors with α', β, δ, and κ-types of conducting layers. They are pseudopolymorphic phases with common chemical formula $(BEDT\text{-}TTF)_4[OsNOCl_5]_{2-x}Solvent_x$.

Organic-inorganic interface interactions play an essential role in these materials. It was shown that the salts can be multicomponent systems when their anion layers include some cation and/or solvent molecules in their composition. This suggests that subtle variations in the structure of the donor layers of these materials and consequently, influence on their transport properties can be achieved by appropriately modifying the nature of their anionic layers. At this point one must take into account that guest solvent molecules can serve as templates but using solvents unfit due to their size, shape, or symmetry creates inevitably disorder and defects to which organic conductors exhibit prominent sensibility. Therefore, special emphasis must be paid to the nature of the guest molecule.

The structural directing role of counterions and guest molecules is of paramount importance because the crucial factor driving the multiplicity of conducting layer types is the docking of the donors onto the layer of anions, *i.e.*, some kind of complementarity of radical cation blocks and counterion units is needed. The studied crystals display a range of remarkable structural features such as conformational and charge ordering in the conducting BEDT-TTF layers as well as commensurate and incommensurate structural modulations mainly related to the positional ordering of the components of complex anion layers.

In this contribution, we present the single-crystal-to-single-crystal transformation (SCSC) from δ-$(BEDT\text{-}TTF)_4[OsNOCl_5]_{1.33}(C_6H_5NO_2)_{0.67}$ salt (**1**) into β''-$(BEDT\text{-}TTF)_3[OsNOCl_5]$ (**2**) induced by a loss of solvent molecules and accompanied by changes in the chemical composition, cell parameters and symmetry, crystal and electronic band structures.

It should be noted, that SCSC transformations with change of the chemical composition generated by release of some molecular components of the crystals have received increasing attention in recent years. The most widely studied transformations involve solvent removal or exchange in porous coordination networks or metal-organic frameworks. Because it is usually difficult to obtain high-quality transformed crystals after removal of solvent due to the collapse of the framework, only a few SCSC transformations have been structurally studied in the case of functional molecular crystals such as molecular magnets or low-dimensional organic conductors [21–25]. Nevertheless, since SCSC-phenomena may lead to modulations in chemical and physical properties, their exploration is very important.

To the best of our knowledge, examples of successful single crystal structural study of SCSC-phenomenon in low-dimensional organic conductors are limited to our investigation of BEDT-TTF polyiodides [25]. It was found that ε-$(BEDT\text{-}TTF)_2I_7$ and ζ-$(BEDT\text{-}TTF)_2I_{10}$ phases easily lose part of the iodine upon heating and transform to β-$(BEDT\text{-}TTF)_2I_3$ with T_c near 7–8 K. It should be noted that the conversion of these phases to the β is accompanied not only by iodine loss, but also by the change in the BEDT-TTF charge state, namely, by the reduction of part of the cations because

the BEDT-TTF charge in ε- and ζ-phases is equal to +1, while it is +0.5 in the β-phase. BEDT-TTF $^{+}$ is likely reduced by the I$^-$ anion formed as a product of the decomposition of the I$_3^-$ anion in the process of solid-phase transformations. The ε→β conversion was monitored by X-ray diffraction on a single crystal of the ε-phase during the process of heat treatment [25–27].

The present study shows the response of the crystal lattice of the δ-(BEDT-TTF)$_4$[OsNOCl$_5$]$_{1.33}$(C$_6$H$_5$NO$_2$)$_{0.67}$ salt to removal of solvent molecules located in the channels between the radical cation BEDT-TTF layers.
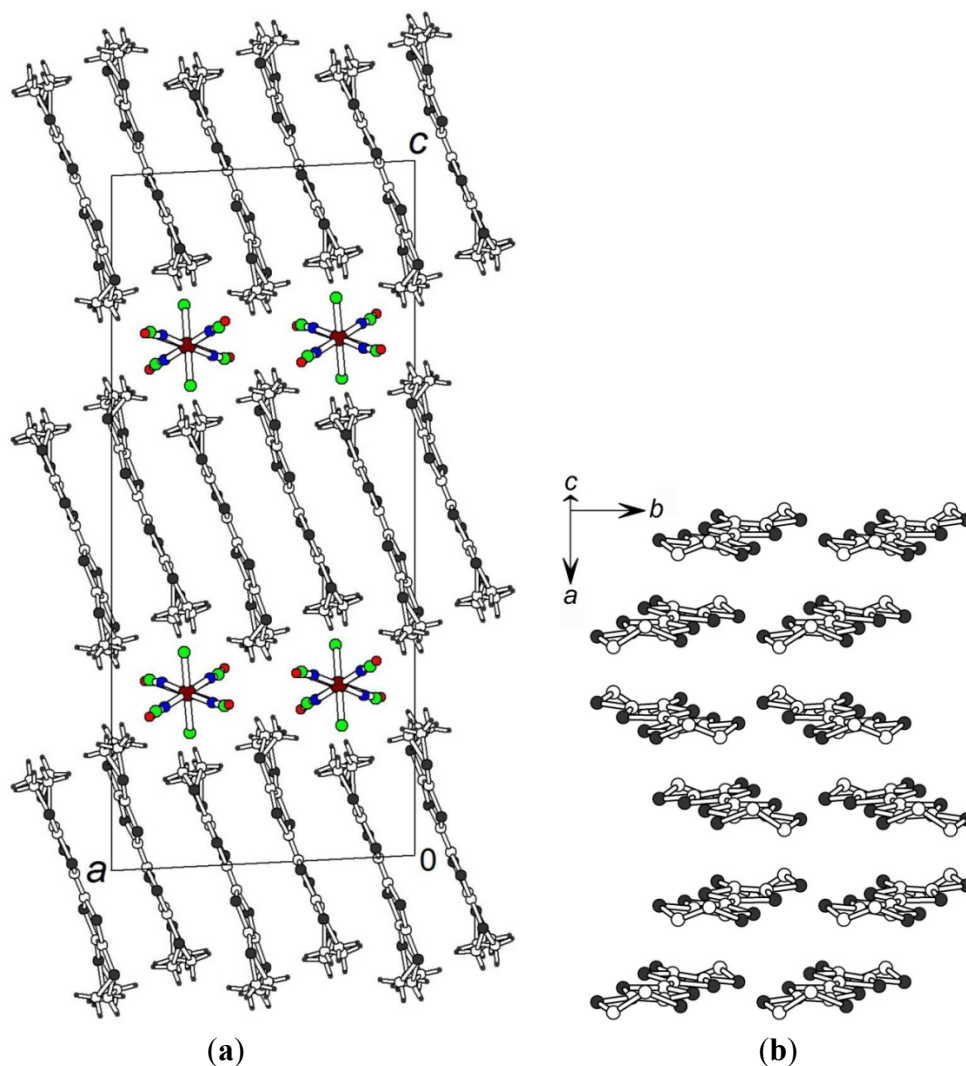
2. Results and Discussion

2.1. Crystal Structures of δ-(BEDT-TTF)₄[OsNOCl₅]₁.₃₃(C₆H₅NO₂)₀.₆₇ (1) and β″-(BEDT-TTF)₃[OsNOCl₅] (2): Different Conducting Layer Packing

The crystal structure of the initial δ-phase (**1**) was described in our previous article [15]. The unit cell of the monoclinic crystal **1** (lattice parameters are given in Table 1) includes two anion layers and two radical cation layers (Figure 1a). There is one independent BEDT-TTF$^{0.67+}$ radical cation in a general position with disorder in both outer ethylene groups. The conducting radical cation layer has a typical δ-type structure. Stacks along the *a*-axis are composed of pairs of parallel BEDT-TTF molecules with a relative turn of the adjacent pairs around the normal to BEDT-TTF molecular planes (Figure 1b). The anion layer has a mixed anion-solvent composition and exhibits strong positional disorder. Nitrobenzene molecules and [OsNOCl$_5$]$^{2-}$ anions occupy the same crystallographic position in a 1:2 ratio (Figure S1 in the Supplementary Information). The octahedral anion sits on an inversion center and its functional nitroso group is disordered in four equiprobable positions. The solvent molecule lies in the plane of nitrosyl ligands and shows disorder in two sites near the inversion center.

Table 1. Unit cell parameters for δ-(BEDT-TTF)$_4$[OsNOCl$_5$]$_{1.33}$(C$_6$H$_5$NO$_2$)$_{0.67}$ (**1**) and β″-(BEDT-TTF)$_3$[OsNOCl$_5$] (**2**).

	δ (1)	β″ (2)
Chemical formula	C$_{44}$H$_{35.33}$Cl$_{6.67}$N$_2$O$_{2.67}$Os$_{1.33}$S$_{32}$	C$_{30}$H$_{24}$Cl$_5$NOOsS$_{24}$
Formula weight	2150.83	1551.39
Crystal system	Monoclinic	Triclinic
a, Å	15.034(3)	7.6672(8)
b, Å	6.728(2)	9.8657(11)
c, Å	35.211(6)	17.9733(12)
α, °	90	91.151(9)
β, °	92.98(1)	93.636(7)
γ, °	90	102.434(9)
V, Å^3	3556(1)	1324.2(2)
Space group, *Z*	*I*2/*a*, 2	$P\bar{1}$, 1

Figure 1. δ-(BEDT-TTF)$_4$[OsNOCl$_5$]$_{1.33}$(C$_6$H$_5$NO$_2$)$_{0.67}$ (**1**). (**a**) View of the structure along *b*. Solvent molecules located in the plane of the disordered NO ligands of the anion are omitted for clarity; (**b**) Donor layer of δ-type projected along [102].

(**a**)　　　　　　　　　　　　(**b**)

With the lapse of time a structural transformation was discovered in the crystals of the δ-phase. This is associated with the changing crystal composition due to loss of the solvent molecules and causes significant structure reorganization. This SCSC transition goes gradually and slowly. An X-ray experiment on freshly prepared crystals showed diffraction from the pure δ-phase. However, at the time of the additional detailed X-ray study, which was performed two years after the crystal syntheses, all the crystals appeared to be composed of two phases: the parent δ-phase and a daughter β″-phase resulting from the transformation. Using a diffractometer equipped with a CCD detector gave an opportunity to recognize clearly in X-ray patterns different sets of diffraction peaks belonging to different phases and to analyze carefully their interrelation. The full array of diffraction intensities was processed with a special option for twinned crystals in the EvalCCD program suite [28].The δ- and β″-phases acted at the integration process as twin domains with different crystal lattice parameters in order to describe more accurately the strongly overlapped reflections from the different phases, but finally the resulting (*hkl*) intensities of each phase were used separately for the structure solution and refinement.

It was found that the δ-phase in the biphasic crystal maintains entirely the monoclinic structure of the pure δ-crystal. The new β″-phase (**2**) has a triclinic structure and the lattice parameters are given in Table 1. Donor and anion layers alternate along the *c*-direction (Figure 2a). The BEDT-TTF layer contains two independent donors: A, in a general position with disorder in one terminal ethylene fragment and B, fully ordered molecule on an inversion center (Figure 2b). The layer has a β″-type molecular packing and consists of BEDT-TTF stacks running along the [1$\bar{1}$0] direction. Central C=C bond lengths analysis in the TTF fragments leads to the conclusion that the positive charge is not uniformly distributed along the stack in contrast to the δ-phase which is built of one independent donor BEDT-TTF$^{0.67+}$. In the β″ structure, donor A with a longer C=C bond of 1.373(9) Å is close to a fully charged radical cation BEDT-TTF$^{\cdot+}$ while molecule B with a shorter C=C bond of 1.345(14) Å is neutral. Calculation of the molecular charge using the empirical formula [29] gives values 0.81+ and 0.15+ for A and B, respectively. Therefore, the molecular sequence in the stack is described as …-A$^{\cdot+}$-A$^{\cdot+}$-B^{0}-A$^{\cdot+}$-A$^{\cdot+}$-B^{0}-… . The sulfur···sulfur intermolecular interactions in the layer are mainly of side-by-side type. They are formed between the neighbor stacks along the [120] direction and the shortest S···S distance is 3.400(3) Å. Interplane separations in the stack are large, 4.03(8) Å (A-A) and 3.9(2) Å (A-B), that prevents existence of notable S···S van der Waals intrastack interactions. Some slightly shortened S···S contacts ≥3.610(3) Å are found inside the step-chains running along [210].

Figure 2. β″-(BEDT-TTF)$_3$[OsNOCl$_5$] (**2**). (**a**) View of the structure along *a*; (**b**) Donor layer of β″-type projected along the long molecular axes where the different intermolecular interactions are labelled; (**c**) Anion layer projected along *c*.

(a)

Figure 2. *Cont.*

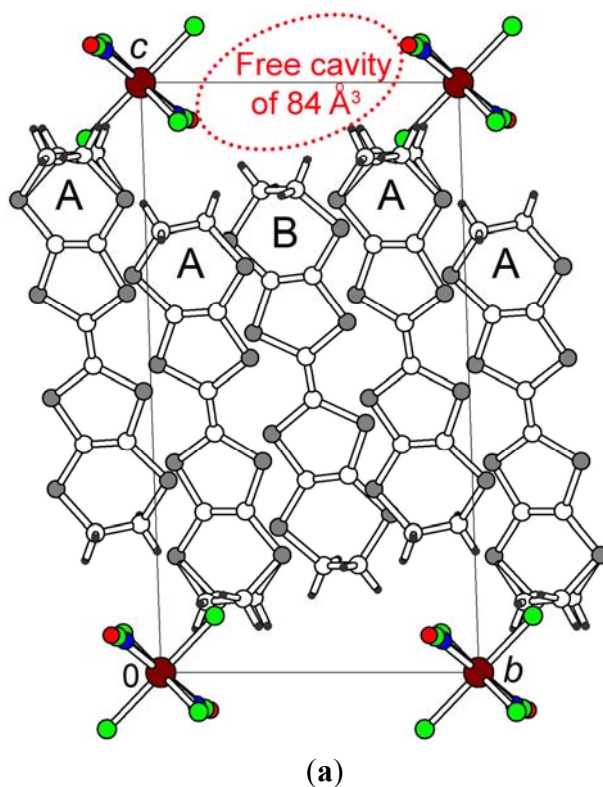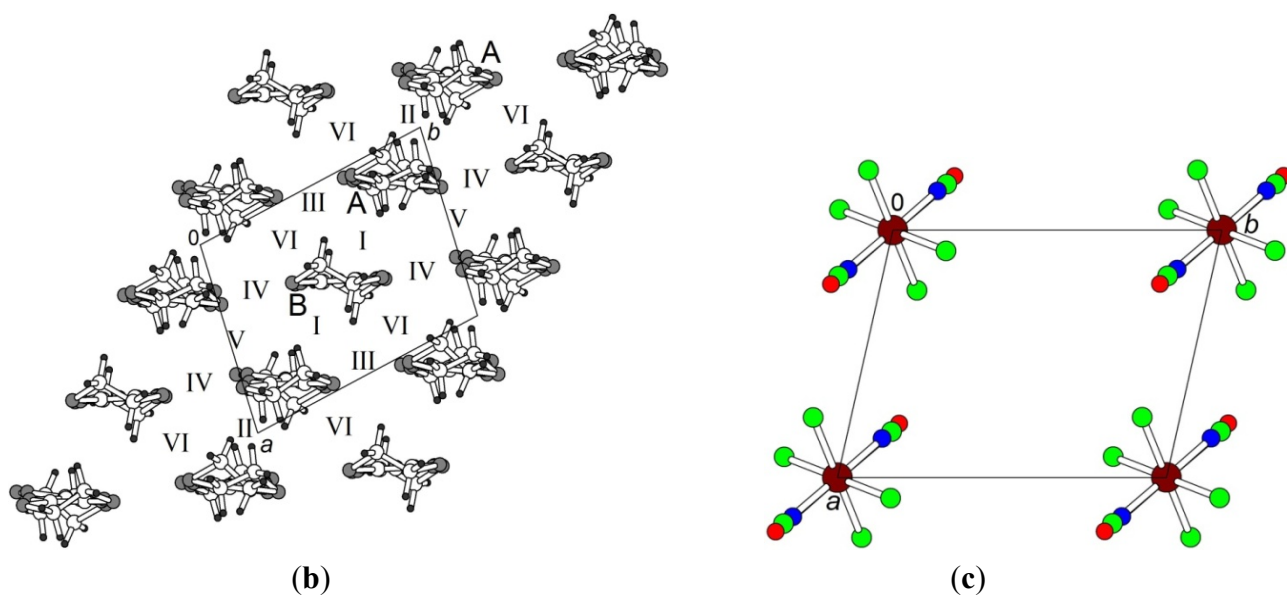(**b**)   (**c**)

Anion layer (Figure 2c) has very simple arrangement from one anion located on an inversion center. The acentric anion still shows a statistical disorder in the positions of the *trans* Cl and NO ligands. Solvent molecules are completely absent in the composition of the new β″-phase while the donor to anion ratio remains unchanged.

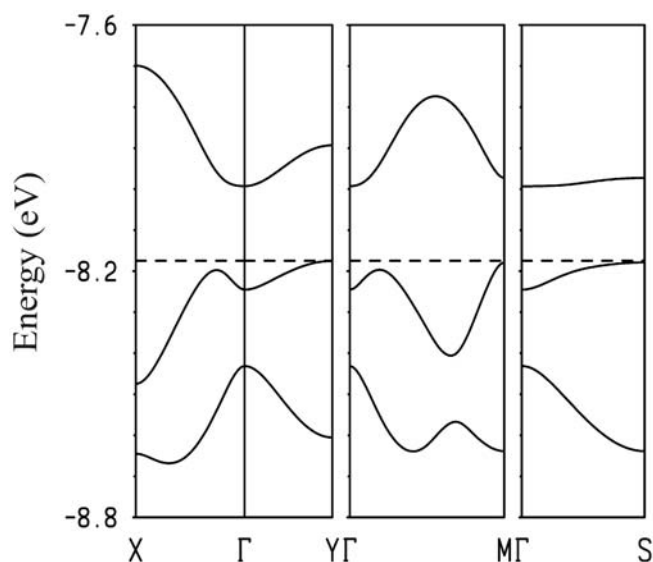*2.2. Electronic Band Structures of δ and β″ Crystals Are very Distinct*

The electronic structure of the δ phase was previously reported [15]. Let us simply recall that the Fermi surface calculated for this phase can be described as a series of superposed rounded rhombuses indicating quasi-two-dimensional metallic properties for the layer of uniformly charged and strongly interacting BEDT-TTF radical cations.

The electronic band structure calculated for a donor layer of β″-(BEDT-TTF)$_3$[OsNOCl$_5$] (Figure 3) exhibits very different features. There are three bands mainly based on the HOMO (highest occupied molecular orbital) of BEDT-TTF because there are three donors per repeat unit of the layer. Since there is one dianion per three donor molecules, the bands in Figure 3 must accommodate two holes. There is a band gap between the two upper bands of this diagram so that this salt must be a regular semiconductor. A more in depth exploration of this aspect was carried out by using a fine mesh of *k*- points inside the Brillouin zone. It was found that the salt should indeed be a semiconductor with an indirect band gap of 0.18 eV.

In order to have a better insight into the origin of the semiconducting behavior, we have analyzed the nature of the different wave vectors for different points of the Brillouin zone and examined the different HOMO⋯HOMO interactions in the donor layers. These layers are shown in Figure 2b where the different intermolecular interactions and donors are labeled. There are two crystallographically non equivalent donors (noted A and B) which are engaged in six different intermolecular interactions (noted I–VI). Two of them are intrastack interactions (I–II), two are lateral π-type interactions (III–IV), and two are σ-type interactions along step-chains (V and VI). The calculated t$_{HOMO-HOMO}$ transfer integrals associated with the six different donor⋯donor interactions as well as the associated S⋯S

contacts are reported in Table 2. It is worth noting that the two HOMO energies are quite different, −8.36 and −8.61 eV for donors A and B, respectively.

Figure 3. Band structure calculated for a donor layer of β"-(BEDT-TTF)$_3$[OsNOCl$_5$]. The dashed line refers to the highest occupied level. Γ = (0, 0), X = ($a*/2$, 0), Y = (0. $b*/2$), M = ($a*/2$, $b*/2$) and S = (-$a*/2$, $b*/2$).

Table 2. $t_{HOMO-HOMO}$ transfer integrals (meV) and S···S distances shorter than 4.0 Å for the different donor···donor interactions in β"-(BEDT-TTF)$_3$[OsNOCl$_5$].

Interaction *	S···S (< 4.0 Å)	$t_{HOMO-HOMO}$ (meV)
I (A-B)	3.837, 3.910	~0
II (A-A)	3.948	−21
III (A-A)	3.458 (x2), 3.480 (x2), 3.826, 3.856 (x2)	−69
IV (A-B)	3.400, 3.485, 3.571, 3.629, 3.877	−27
V (A-A)	3.610 (x2), 3.644 (x2), 3.658 (x2), 3.939	+229
VI (A-B)	3.654, 3.722, 3.765, 3.796, 3.945, 3.960, 3.986	+78

* Intermolecular interactions I–VI are labelled in Figure 2b.

Analysis of the wave vectors for different points of the Brillouin zone clearly shows that the lower of the three HOMO bands is largely concentrated on the HOMO of donor B. In contrast the two upper bands are mostly built from the HOMO of donor A. Since the upper band of this pair is empty, donor A can be considered as being positively charged whereas donor B can be formally considered as neutral. Of course this is in harmony with the considerably lower energy of the HOMO of donor B. In other words, as far as the HOMO···HOMO interactions are concerned, the donor layers of this salt can be described as a series of (A-A)$^{2+}$ dimers interacting directly or through neutral B donors. However, what the data of Table 2 reveals is that even if the stacks are of the type ···B-A-A-B-A-A-B···, the dimers are not the A-A pairs in the stacks because this interaction is quite weak. The A-A interaction along the step-chains direction is by far the stronger HOMO···HOMO interaction of the layer and consequently qualifies the associated pair as the dimeric units of the layer. In view of the transfer

integrals of Table 2 it is clear that these (A-A)$^{2+}$ dimers interact directly through interaction III or through the neutral donors (B) as a result of interaction VI. The other interactions are clearly weaker.

In view of these results it is clear that the main feature behind the existence of a band gap in this material is the strong dimerization along the step-chains direction. The strong energy gap arising from the dimerization cannot be closed by the direct or indirect dimer⋯dimer interactions which are responsible for the spread of the two dimeric levels into the two upper bands. Thus the simplest way to decrease the band gap and maybe lead to a metallic type behavior for salts with this structure would be to make the interactions along the step-chains direction more uniform.

The room temperature conductivity of salt **1** is 1 S cm^{-1} and it grows very weakly down to about 160 K and then it begins to drop sharply indicating a metal-to-insulator transition [15]. It was impossible to measure the conductivity of the salt **2** because of the absence of a single-phase sample due to incomplete δ to β″ conversion. However, both the crystal and electronic structures of the δ and β″ radical cation salts are suggestive of a transition of crystal conductivity from metallic to activated type.
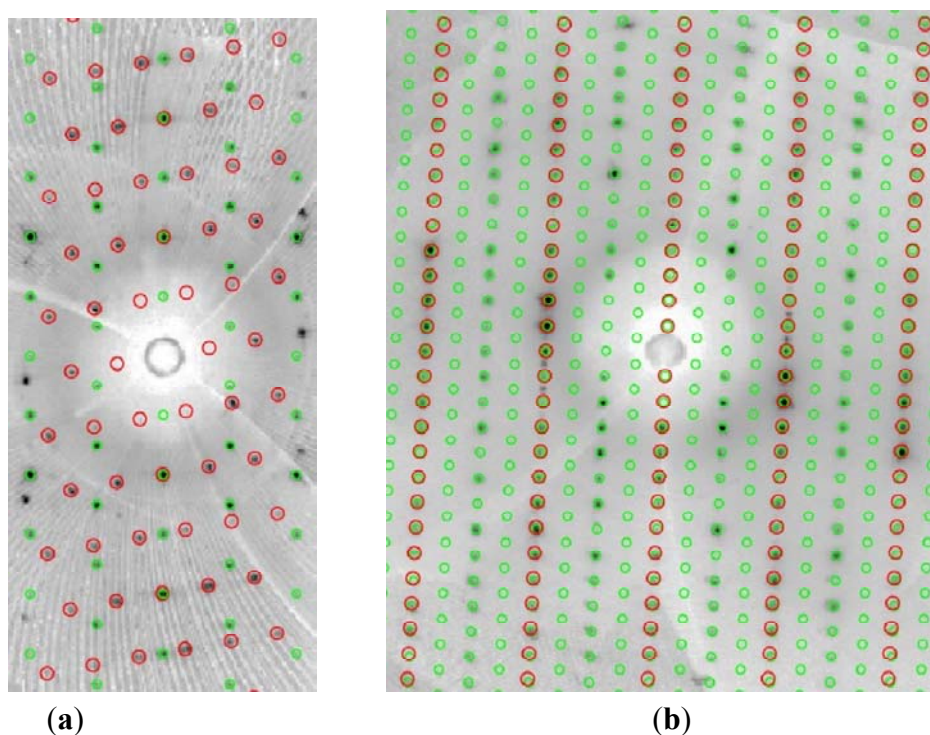
2.3. On the Origin of SCSC Transformation: Huge Structural Changes in both the Donor and Anion Layers

The coexistence of two phases, δ and β″, in the same crystal gives a rare opportunity to specify the exact mutual orientation of the lattices before and after the transition and reveal a mechanism for the structural transformation. It should be noted that most of the crystals show twinning of the β″-phase: the monoclinic axis of the parent δ-structure survives as a twin operation in the triclinic β″-structure after the transition, this is the usual case for organic molecular compounds with weak (mainly van der Waals) intermolecular interactions. We were lucky to find the sole crystal without twinning for X-ray study. Diffraction images from this crystal contain just two systems of reflections: one from the δ-phase and another from the β″-phase. Figure 4a represents the $(hk0)_\delta$ plane of the reciprocal space reconstructed from the experimental diffraction data, as an example. Reflections belonging to different phases are outlined by different circles: small green for δ and big red for β″, respectively. The transformation matrix from δ to β″ is (0.50, 0.20, 0; −0.25, 1.35, 0; 0 −0.12, 0.50). Owing to a distortion of the lattice at the transition, overlapping of the two lattices is not very extensive (~15%). The maximal overlap is observed in the $(h0l)_\delta$ reciprocal plane (Figure 4b): rows of reflections $(h0l)_\delta$ with $h = 4n$ from δ-lattice are superposed with $(hkl)_{\beta''}$ reflections from the β″-lattice with $k = n$, $h = 2k$.

At the transition, reorganization of the molecular packing occurs within the conducting donor layers. Figure 5 shows a schematic diagram of the BEDT-TTF layer transformation. The initial δ-type layer (Figure 5a) already contains the fragments identical to β″-packing–double slabs of parallel BEDT-TTF molecules which remain essentially rigid during the transition while all the molecules in the adjacent double slabs must be turned by ~30° in the plane of slab to achieve the β″-arrangement. The layer fragment where reorientation of BEDT-TTF molecules occurs is framed in Figure 5a. This structure transformation is significant because the character of molecular interactions between the double slabs switches from twist to parallel (Figure 5c,d, respectively). To realize how this grandiose transformation becomes possible, one should analyze the interslab interactions. The interplanar separation between BEDT-TTF slabs in δ-layer are quite large (3.7 Å) and intermolecular S⋯S contacts shorter than the sum of the van der Waals radii are generated only between neighboring
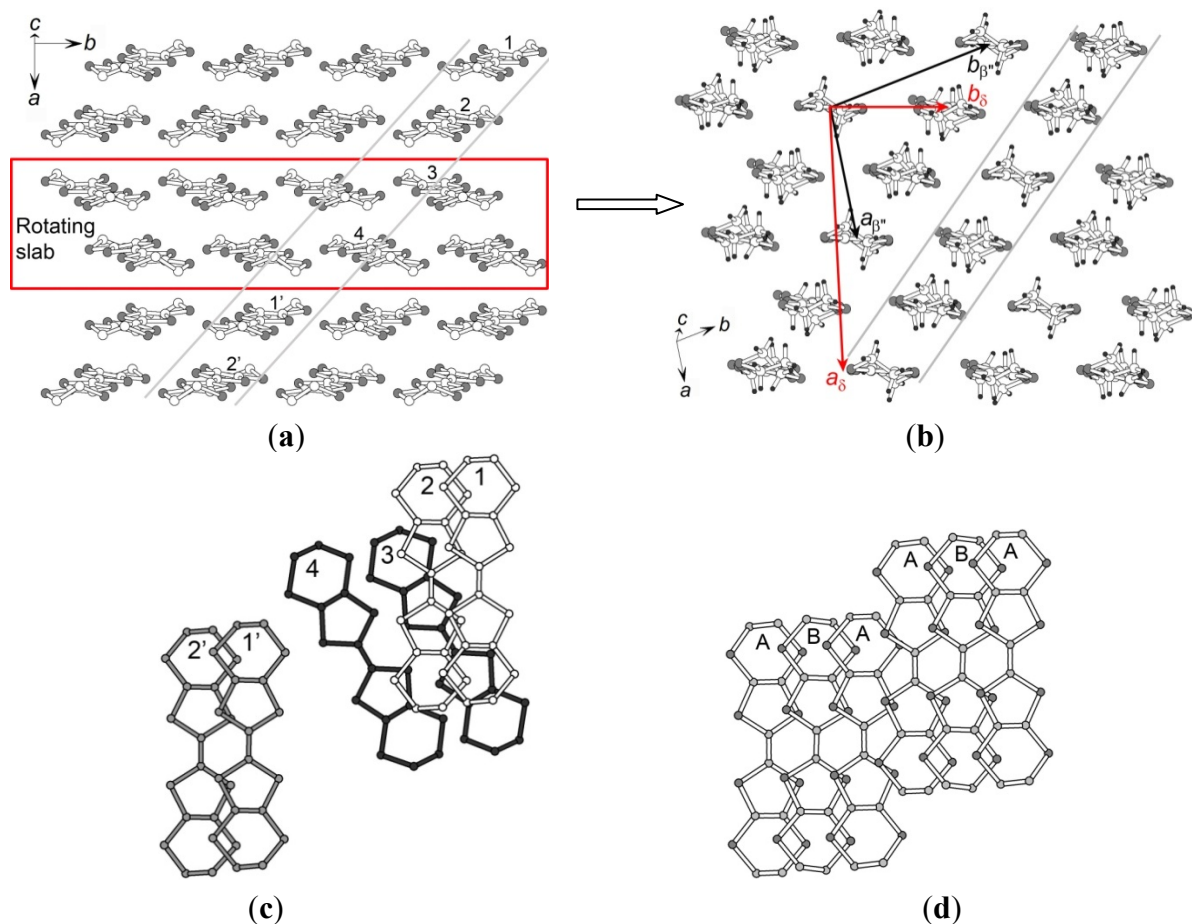
stacks along the *b*-direction, *i.e.*, inside the slabs (S⋯S distances are 3.473–3.576(3) Å), while between the slabs all S⋯S distances exceed 3.68 Å. In the β″-phase the interplanar separations in the stack become even larger, 3.9–4.0 Å. Apparently, the rotating double BEDT-TTF slab weakly interacts with adjacent, non moving slabs providing a possibility for synchronic molecular rotation and facilitates a sliding of BEDT-TTF slabs during the transition. Note, that the repeat unit of the stack includes three BEDT-TTF in β″ instead of four molecules in δ. Comparison of Figure 5c,d leads to the conclusion that there is an additional relative shift of the molecules which makes the stack in the β″-layer more compact in two directions: along both longitudinal and transversal axes of BEDT-TTF, while in the third direction, normal to the BEDT-TTF mean plane, the intermolecular separation increases.

Figure 4. (**a**) $(hk0)_\delta$; and (**b**) $(h0l)_\delta$ planes of the reciprocal space reconstructed from the experimental X-ray data. Diffraction reflections corresponding to two different lattices, δ and β″, are shown in small green and big red circles, respectively.
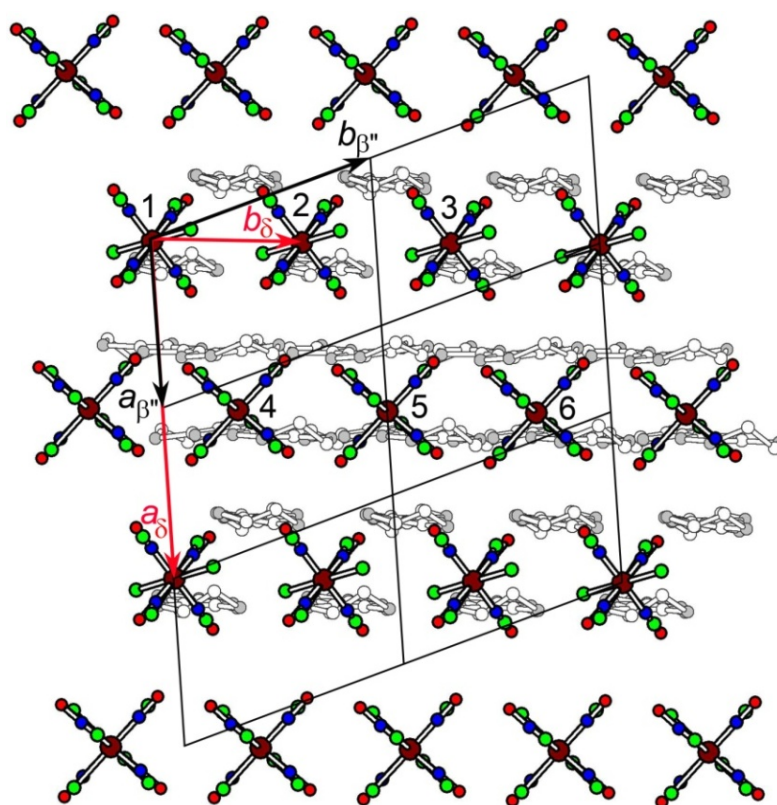

(**a**)   (**b**)

The anion layer undergoes drastic, striking changes during the transition. A projection of the anion layer in the δ-phase and a scheme of the anion lattice in the β″-phase are shown in Figure 6; there the adjacent donor layer is drawn in the background to show the relative orientation of anions and donors. Each anion position in the δ-lattice is occupied by a 2:1 mixture of the anion and solvent, the solvent molecules are omitted for clarity in this figure. All vertices of the β″-lattice shown by black solid lines in Figure 6 are fully occupied by the anions after the SCSC transformation (Figure 2c). One can see that only every sixth anion of δ-phase (marked by number 1 in Figure 6) keeps its initial spatial position in the β″-structure. Solvent molecules completely disappear and the rest of the anions (numbered as 2–6) show strong shifts to achieve the positions of the β″-lattice. At first sight the anion layer reorganization seems to be even more mysterious than the strong donor movement.

Figure 5. Scheme of the δ to β" transformation. Rotation of a double BEDT-TTF slab in the δ-layer (**a**) leads to formation of the β"-layer (**b**). Directions of the lattice axes in δ- and β"-structures are shown in (**b**) by red and black arrows, respectively. Overlaps of the molecules inside the stacks defined by grey lines in (**a**) and (**b**) are presented in (**c**) and (**d**), respectively.

(**a**)

(**b**)

(**c**)

(**d**)

It is obvious that large freedom for molecular displacement inside the anion layer is necessary for the δ→β" transformation. A major precondition for the strong anionic motion can already be found in the structure of the initial δ-phase. As is seen in Figure 1, the terminal ethylene groups of several BEDT-TTF molecules form channels along the monoclinic *b*-axis which include the anions $[OsNOCl_5]^{2-}$ in a mixture with nitrobenzene molecules. In spite of a great number of C-H···Cl and C-H···O short contacts between the cation and anion sublattices, some kind of a "melting" of the anionic chains is observed, resulting in anion movement along the channels and appearance of the superstructure.

Figure 6. Anion layer in the δ-structure with neighbor donor layer in the background and scheme of the β"-lattice drawn as black solid lines. (Note, that in fact a$_{β''}$ and a$_δ$ axes are not exactly co-directed: correct directions are shown in Figure 5b. The lattice distortion leading to deviation of the $a_{β''}$-axis from the initial direction of the $a_δ$-axis occurs simultaneously for donor and anion layers and is not shown here to avoid too much complexity in the figure. Besides, in this "idealized" orientation of the $a_{β''}$-axis, the relation between the anion sublattices in the δ- and β"-structures becomes more obvious.)

An X-ray structural study was carried out on δ-type crystals **1** from two identical electrochemical syntheses. In the crystals from one of two batches a commensurate superstructure was observed. Additional weak and diffuse diffraction peaks correspond to triplication of the shortest lattice translation *b*, 6.73 Å × 3 = 20.2 Å (Figures S2 and S3a in the Supplementary Information). The detailed study of the superstructure was complicated by the presence in the crystal of a non-merohedrically twinned β"-phase in addition to the δ one. This crystal sample gave a very complex X-ray diffraction pattern which can be fitted by three lattices, diffraction peaks from twin β"-lattices intersecting with both main and superstructural reflections of δ-lattice. Data processing and structure refinement in the triple δ-lattice were attempted. Although only rough results were obtained which are described in the Supplementary Information, some general conclusions can still be made. First, including superstructural peaks in the calculations did not lead to an ordered anion layer although one could expect complete ordering of two anions and one solvent molecule on the triple period of 20.2 Å. Instead, disordered anion chains containing partially occupied anion positions with alternating Os-Os distances of 3.2 and 6.8 Å are found along the triple *b* axis. Anion sites occupation and mutual displacement of the neighbor anion chains are found to differ in two independent anion layers (Figure S4 in the Supplementary Information). On the basis of these facts one can conclude that the

components of the mixed anion-solvent chains seem to be very mobile and, furthermore, adjacent chains in the anion layer are weakly sensitive to each other and can move independently. Thus, the rough structural model allows an explanation of the appearance of the superstructure by displacement of the anions from their average positions (shown in Figure 6) along the direction of triple translation.

It should be noted, that the anion and solvent movement along the chains is just a necessary but not sufficient condition for the observed anion sublattice transformation. The latter can be described as a complex process combining several stages. In the first stage, constituents of the anion layer move along the b_δ-axis at the same time that the nearest BEDT-TTF double slab turns. In the second stage a shift of the anions along the a_δ-axis is also necessary to reach the correct positions in the anion lattice of the β"-phase (Figure 6). It was found that less tight molecular packing is achieved in the β"-structure than in the δ-one. The cell volume corresponding to one formula unit of δ-$(BEDT-TTF)_4[OsNOCl_5]_{1.33}(C_6H_5NO_2)_{0.67}$ decreases at the transition by only 12.4 $Å^3$ whereas the molecular volume of the vanishing $0.67(C_6H_5NO_2)$ is about 100 $Å^3$. As a result, the β"-lattice contains large and continuous free cavities in the anion layer with maximum cross-section near the (0, 1/2, 0) inversion center (Figure 2a). The volume of the cavity, 84 $Å^3$, is smaller than the volume of the solvent. However, it seems that the solvent uses these free channels along *a* to go out of the crystal. Thus, anions and solvent move along the *b*-chains, and simultaneously additional channels along the *a*-axis open up, enabling anions to reach the new positions and solvent molecules to leave the crystal.

3. Experimental Section

3.1. X-ray Diffraction

Single crystal X-ray diffraction experiments were performed on crystals from two similar syntheses (batches A and B). All freshly prepared crystals showed diffraction from the pure δ-$(BEDT-TTF)_4[OsNOCl_5]_{1.33}(C_6H_5NO_2)_{0.67}$ phase [15]. The initial task of the additional X-ray study was the investigation of the superstructure which was detected on Weissenberg photographs of the crystals from batch A while in the crystals from batch B such superstructure was not observed. In the course of the new X-ray experiments carried out two years after the crystal syntheses, it was found that in all the crystals a partial single-crystal-to-single-crystal conversion occurred over time. CCD images contained diffraction reflections from the parent δ-phase in combination with peaks from the new β"-phase indicating the presence of both phases in all the crystals from batches A and B; the superstructure was still present in the crystals from batch A.

Full sets of the X-ray data for crystals from both syntheses were collected at room temperature on a Bruker Nonius KappaCCD diffractometer with MoK_α radiation (λ = 0.71073 Å, graphite monochromator) using the combined φ- and ω-scan method. Little space intersection of the reflections from δ-and β"-lattices allowed successful procession of the data. Intensities of diffraction peaks from different lattices were integrated using special twin option in EvalCCD program suite [28] but collected in different hkl-files, separately for each lattice. Empirical absorption correction of experimental intensities was applied using the SADABS program [30].

The structure of the β"-phase was solved for crystals from batch B by a direct method followed by Fourier syntheses and refined by a full-matrix least-squares method using the SHELX-97 programs [31]. All non-hydrogen atoms were refined in an anisotropic approximation, except for a

disordered NO group of the anion. H atoms were placed in idealized positions and refined using a riding model with U_{iso}(H) fixed at $1.2U_{eq}$(C). The main crystal data are listed in Table 1. Refinement data: $D_{calc} = 1.945$ g cm^{-3}, $\mu = 36.38$ cm^{-1}, $2\Theta_{max} = 54.98°$, reflections measured 26451, unique reflections 5653 ($R_{int} = 0.0539$), reflections with $I > 2\sigma(I) = 4608$, parameters refined 304, $R_1 = 0.0475$, $wR_2 = 0.1277$, GOF = 1.083. CCDC-871314 contains the supplementary crystallographic data for **2**. These data can be obtained free of charge from The Cambridge Crystallographic Data Centre via www.ccdc.cam.ac.uk/data_request/cif.

For the crystal from batch A, determination and analysis of the crystal structure of the δ-phase in the triple lattice taking into account the satellite reflections were attempted. The results are described in the Supplementary Information.

3.2. Electronic Band Structure Calculations

The tight-binding band structure calculations [32] were of the extended Hückel type. A modified Wolfsberg-Helmholtz formula was used to calculate the non-diagonal $H_{\mu\nu}$ values [33]. All valence electrons were taken into account in the calculations and the basis set consisted of Slater-type orbitals of double-ζ quality for C 2s and 2p, S 3s and 3p and of single-ζ quality for H1s. The ionization potentials, contraction coefficients and exponents were taken from previous work [34].

4. Conclusions

In conclusion, we have found that single crystals of δ-(BEDT-TTF)$_4$[OsNOCl$_5$]$_{1.33}$(C$_6$H$_5$NO$_2$)$_{0.67}$ (**1**) are partially converted over time into a new chemical entity, β"-(BEDT-TTF)$_3$[OsNOCl$_5$] (**2**), without loss of crystallinity in spite of the large molecular movements occurring during the transformation. The SCSC transformation is associated with huge changes in the structure: the donor layer switches out of its packing mode, something which should have a dramatic influence on conductivity, while in the anion layer the neutral solvent molecules leave and a large concerted displacement of the anions occurs. Most likely, this is a transition from a metastable phase to a more stable one and changing the composition of the crystal predetermines the irreversible character of the structural transformation. These phenomena are of significant interest in terms of crystal engineering and materials science. The β"-salt resulting from the SCSC conversion is a new phase in the family of organic molecular conductors combining BEDT-TTF and [OsNOCl$_5$]$^{2-}$ anions along with the previously studied α', β, δ, and κ-phases.

References

1. Kushch, L.; Buravov, L.; Tkacheva, V.; Yagubskii, E.; Zorina, L.; Khasanov, S.; Shibaeva, R. Molecular metals based on radical cation salts of ET and some its analogues with the photochromic nitroprusside anion, $[Fe(CN)_5NO]^{2-}$. *Synthet. Metal.* **1999**, *102*, 1646–1649.

2. Gener, M.; Canadell, E.; Khasanov, S.S.; Zorina, L.V.; Shibaeva, R.P.; Kushch, L.A.; Yagubskii, E.B. Band structure and Fermi surface of the $(BEDT-TTF)_4M[Fe(CN)_5NO]_2$ (M = Na, K, Rb,...) molecular metals contaning the photochromic nitroprusside anion. *Solid State Commun.* **1999**, *111*, 329–333.

3. Clemente-León, M.; Coronado, E.; Galán-Mascarós, J.R.; Giménez-Saiz, C.; Gómez-Garcia, C.J.; Fabre, J.M. Molecular conductors based upon TTF-type donors and octahedral magnetic complexes. *Synthet. Metal.* **1999**, *103*, 2279–2282.

4. Clemente-León, M.; Coronado, E.; Galán-Mascarós, J.R.; Gómez-Garcia, C.J.; Canadell, E. Hybrid molecular materials based upon the photochromic nitroprusside complex, $[Fe(CN)_5NO]^{2-}$, and organic π-electron donors. Synthesis, structure, and properties of the radical salt $(TTF)_7[Fe(CN)_5NO]_2$ (TTF = Tetrathiafulvalene). *Inorg. Chem.* **2000**, *39*, 5394–5397.

5. Zorina, L.V.; Khasanov, S.S.; Shibaeva, R.P.; Gener, M.; Rousseau, R.; Canadell, E.; Kushch, L.A.; Yagubskii, E.B.; Drozdova, O.O.; Yakushi, K. A new stable organic metal based on the BEDO-TTF donor and the doubly charged nitroprusside anion, $(BEDO-TTF)_4[Fe(CN)_5NO]$. *J. Mater. Chem.* **2000**, *10*, 2017–2023.

6. Khasanov, S.S.; Zorina, L.V.; Shibaeva, R.P. Structure of organic metals based on BEDT-TTF with photochromic nitroprusside anion, $(BEDT-TTF)_4M[Fe(CN)_5NO]_2$ where M = Na^+, K^+, NH_4^+, Tl^+, Rb^+, Cs^+. *Russ. J. Coord. Chem.* **2001**, *27*, 259–269.

7. Clemente-León, M.; Coronado, E.; Galán-Mascarós, J.R.; Giménez-Saiz, C.; Gómez-Garcia, C.J.; Ribera, E.; Vidal-Gancedo, J.; Rovira, C.; Canadell, E.; Laukhin, V. Hybrid molecular materials based upon organic π-electron donors and metal complexes. Radical salts of bis(ethylenethio)tetrathiafulvalene (BET-TTF) with the octahedral anions hexacyanoferrate(III) and nitroprusside. The first kappa phase in the BET-TTF family. *Inorg. Chem.* **2001**, *40*, 3526–3533.

8. Sanchez, M.-E.; Doublet, M.-L.; Faulman, C.; Malfant, I.; Cassoux, P.; Kushch, L.; Yagubskii, E. Anion conformation and physical properties in BETS salts with the nitroprusside anion and its related ruthenium halide (X = Cl, Br) mononitrosyl complexes: θ-$(BETS)_4[Fe(CN)_5NO]$, $(BETS)_2[RuBr_5NO]$ and $(BETS)_2[RuCl_5NO]$. *Eur. J. Inorg. Chem.* **2001**, *11*, 2797–2804.

9. Shevyakova, I.Y.; Buravov, L.I.; Kushch, L.A.; Yagubskii, E.B.; Khasanov, S.S.; Zorina, L.V.; Shibaeva, R.P.; Drichko, N.V.; Oleinischak, I. Radical cation salts of TTT and TSeT with photochromic anion $[FeNO(CN)_5]^{2-}$. *Russ. J. Coord. Chem.* **2002**, *28*, 487–495.

10. Zorina, L.V.; Gener, M.; Khasanov, S.S.; Shibaeva, R.P.; Canadell, E.; Kushch, L.A.; Yagubskii, E.B. Crystal and electronic structures of the radical cation salt based on EDT-TTF and the photochromic nitroprusside anion, $(EDT-TTF)_3[Fe(CN)_5NO]$. *Synthet. Metal.* **2002**, *128*, 325–332.

11. Shevyakova, I.Y.; Zorina, L.V.; Khasanov, S.S.; Buravov, L.I.; Tkacheva, V.A.; Shibaeva, R.P.; Yagubskii, E.B.; Canadell, E. The first mixed valence radical cation salts of BEDT-TTF with the

photochromic metal mononitrosyl complexes $[RuNOX_5]^{2-}$ (X = Br, Cl) as counterions. *J. Solid State Chem.* **2002**, *168*, 514–523.

12. Shibaeva, R.P.; Yagubskii, E.B.; Canadell, E.; Khasanov, S.S.; Zorina, L.V.; Kushch, L.A.; Prokhorova, T.G.; Shevyakova, I.Y.; Buravov, L.I.; Tkacheva, V.A.; *et al.* Structure-properties relationships in organic molecular conductors based on radical cation salts with octahedral metal complexes as counterions. *Synthet. Metal.* **2003**, *133–134*, 373–375.

13. Shevyakova, I.; Buravov, L.; Tkacheva, V.; Zorina, L.; Khasanov, S.; Simonov, S.; Yamada, J.; Canadell, E.; Shibaeva, R.; Yagubskii, E. New organic metals based on BDH-TTP radical cation salts with the photochromic nitroprusside anion $[FeNO(CN)_5]^{2-}$. *Adv. Funct. Mater.* **2004**, *14*, 660–668.

14. Zorina, L.V.; Khasanov, S.S.; Shibaeva, R.P.; Shevyakova, I.Y.; Kotov, A.I.; Yagubskii, E.B. Crystal structure of the new radical cation salt $(DOET)_4[Fe(CN)_5NO]_{1.25}(C_6H_5Cl)_{0.75}$. *Crystallogr. Rep.* **2004**, *49*, 1010–1017.

15. Simonov, S.V.; Shevyakova, I.Y.; Zorina, L.V.; Khasanov, S.S.; Buravov, L.I.; Emel'yanov, V.A.; Canadell, E.; Shibaeva, R.P.; Yagubskii, E.B. Variety of molecular conducting layers in the family of radical cation salts based on BEDT-TTF with the metal mononitrosyl complex $[OsNOCl_5]^{2-}$. *J. Mater. Chem.* **2005**, *15*, 2476–2488.

16. Zorina, L.V.; Khasanov, S.S.; Simonov, S.V.; Shibaeva, R.P.; Kushch, L.A.; Buravov, L.I.; Yagubskii, E.B.; Boudron, S.; Méziere, C.; Batail, P.; *et al.* Crystalline patterns and band structure dimensionality in a series of conducting hybrids associating amide-functionalized EDT-TTF π-donors with the isosteric octahedral anions $[FeNO(CN)_5]^{2-}$ and $[M(CN)_6]^{3-}$ (M = Co, Fe)". *Synthet. Metal.* **2005**, *155*, 527–538.

17. Simonov, S.V.; Zorina, L.V.; Khasanov, S.S.; Shibaeva, R.P.; Shevyakova, I.Y.; Buravov, L.I.; Yagubskii, E.B.; Canadell, E. Molecular conductors with the common and robust building block $(BEDT-TTF)_2NP$ (NP = $[FeNO(CN)_5]^{2-}$) but different band filling. *J. Mater. Chem.* **2006**, *16*, 787–794.

18. Shibaeva, R.P.; Khasanov, S.S.; Zorina, L.V.; Simonov, S.V. Structural Features of Low-dimensional molecular conductors—representatives of new hybrid polyfunctional materials: Review. *Crystallogr. Rep.* **2006**, *51*, 949–967.

19. Zorina, L.V.; Simonov, S.V.; Khasanov, S.S.; Shibaeva, R.P. Pseudopolymorphism, superstructure, and phase transitions in the crystals of $(BEDT-TTF)_4[MNOX_5]_{2-x}G_x$ molecular conductor family, where M = Os, Ru; X = Cl, Br; G is a solvent molecule. *J. Struct. Chem.* **2009**, *50*, S152–S159.

20. Zorina, L.V.; Simonov, S.V.; Khasanov, S.S.; Shibaeva, R.P.; Suslikova, I.Y.; Kushch, L.A.; Yagubskii, E.B. Crystal structure of the new organic conductor $(TSeF)_7[FeNO(CN)_5]_2$ with unusual molecular packing of conducting layer. C*rystallogr. Rep.* **2011**, *56*, 1111–1115.

21. Hao, Z.M.; Zhang, X.M. Solvent induced molecular magnetic changes observed in single-crystal-to-single-crystal transformation. *Dalton Trans.* **2011**, *40*, 2092–2098.

22. Kurmoo, M. Magnetic metal-organic frameworks. *Chem. Soc. Rev.* **2009**, *38*, 1353–1379.

23. Maspoch, D.; Ruiz-Molina, D.; Veciana, J. Magnetic nanoporous coordination polymers. *J. Mater. Chem.* **2004**, *14*, 2713–2723.

24. Song, Y.; Luo, F.; Luo, M.; Liao, Z.; Sun, G.; Tian, X.; Zhu, Y.; Yuan, Z.J.; Liu, S.; Xu, W.; *et al*. The application of single-crystal-to-single-crystal transformation towards adjustable SMM properties. *Chem. Commun.* **2012**, *48*, 1006–1008.

25. Shibaeva, R.P.; Yagubskii, E.B. Molecular conductors and superconductors based on trihalides of BEDT-TTF and some of its analogues. *Chem. Rev.* **2004**, *104*, 5347–5378.

26. Zvarykina, A.V.; Kononovich, P.A.; Laukhin, V.N.; Molchanov, V.N.; Pesotskii, S.I.; Simonov, V.I.; Shibaeva, R.P.; Schegolev, I.F.; Yagubskii, E.B. Nature of the high-temperature superconducting state with T_c =7–8 K in β-(BEDT-TTF)$_2$I$_3$. *JETP Lett.* **1986**, *43*, 329–332.

27. Shibaeva, R.P.; Yagubskii, E.B.; Laukhina, E.E.; Laukhin, V.N. *The Physics and Chemistry of Organic Superconductors*; Saito, G., Kagoshima, S., Eds.; Springer-Verlag: Berlin, Germany, 1990; p. 342.

28. Duisenberg, A.J.M.; Kroon-Batenburg, L.; Schreurs, A.M.M. Intensity evaluation method. *J. Appl. Cryst.* **2003**, *36*, 220–229.

29. Guionneau, P.; Kepert, C.J.; Bravic, G.; Chasseau, D.; Truter, M.R.; Kurmoo, M.; Day, P. Determining the charge distribution in BEDT-TTF salts. *Synthet. Metal.* **1997**, *86*, 1973–1974.

30. Sheldrick, G.M. *SADABS*: *Program for Empirical Absorption Correction of Area Detector Data*; University of Göttingen: Göttingen, Germany, 1996.

31. Sheldrick, G.M. A short history of SHELX. *Acta Crystallogr. Sect. A* **2008**, *64*, 112–122.

32. Whangbo, M.-H.; Hoffmann, R. The band structure of the tetracyanoplatinate chain. *J. Am. Chem. Soc.* **1978**, *100*, 6093–6098.

33. Ammeter, J.H.; Bürgi, H.B.; Thibeault, J.C.; Hoffmann, R. Counterintuitive orbital mixing in semiempirical and ab initio molecular orbital calculations. *J. Am. Chem. Soc.* **1978**, *100*, 3686–3692.

34. Pénicaud, A.; Boubekeur, K.; Batail, P.; Canadell, E.; Auban-Senzier, P.; Jérome, D. Hydrogen-bond tuning of macroscopic transport properties from the neutral molecular component site along the series of metallic organic-inorganic solvates (BEDT-TTF)$_4$Re$_6$Se$_5$Cl$_9$·[guest], [guest = DMF, THF, dioxane]. *J. Am. Chem. Soc.* **1993**, *115*, 4101–4112.